APPLIED BIOCHEMISTRY AND BIOTECHNOLOGY 6, 91-117 (1981)

Entrapment of Living Microbial Cells in Covalent Polymeric Networks

II. A Quantitative Study on the Kinetics of Oxidative Phenol Degradation by Entrapped *Candida tropicalis* Cells

JOACHIM KLEIN* AND PETER SCHARA†

Institute of Chemical Technology, Technical University of Braunschweig, Hans-Sommer-Str. 10, D 3300 Braunschweig, Federal Republic of Germany

Received January 18, 1980; Accepted August 18, 1980

Abstract

The kinetics of oxidative phenol degradation with microbial cells *Candida tropicalis*, immobilized in a polyacrylamide and polymethacrylamide matrix, were mathematically simulated assuming zero-order and Michaelis-Menten rate equations.

For zero-order kinetics an expanded equation for catalytic effectiveness as a function of the Thiele modulus, Biot number, and partition coefficients was derived and compared with numerical solutions for Michaelis-Menten kinetics. Errors with regard to the zero-order approximation become negligible if $c_0/K_M > 2$.

Experimentally determined catalyst activities as a function of particle size and cell concentration were compared to calculated ones. Additional experiments to determine the diffusion and oxygen consumption ratios have been carried out in an effort to resolve the physical parameters to be used in the above mentioned calculations.

Furthermore, experiments on cell growth during reincubation with nutrients and oxygen are reported; an increase in activity up to a factor of ten was

†Present address: Degussa, ZN Wolfgang, D 6450 Hanau, Federal Republic of Germany.

0273-2289/81/0600-0091$05.40

observed. These experiments demonstrate that the microbial cells are entrapped in the polymer matrix in the living state.

Index Entries: *Candida tropicalis*, entrapped; microbes, entrapped living; immobilized microbes, living; polymeric networks, entrapped microbes in; phenol degradation; kinetics, with entrapped cells; catalytic efficacy, mathematical calculation of; fermentation, of entrapped cells.

1. Introduction

In the preceding paper (*1*), different types of polyreactions have been compared to develop improved procedures for whole-cell immobilization via polymer entrapment. Choosing dibutyl phthalate as the suspending liquid, polyacrylamide beads could be prepared with a retention of catalytic cell activity of close to 100%. By substituting acrylamide (AAm) with methacrylamide (MAAm), polymer networks of improved mechanical stability could be obtained.

In this preceding publication, "catalytic activity" was referred to only in a qualitative manner to obtain a general idea of toxic inactivation during cell immobilization.

As is well known in heterogeneous catalysis, the activity of such a system is not only a function of the concentration of active sites, but also depends on the supply of substrates to these sites. A complete analysis of the "catalytic activity" problem therefore requires not only information on the reaction kinetics themselves, but also on the diffusional transport and partition equilibria. This approach through analogy to heterogeneous catalysis has long been realized in bioengineering systems, e.g., in immobilized enzyme catalysis (*2–6*, *14*) or pelletal growth.

In studying phenol degradation with immobilized *Candida tropicalis* cells we soon realized the necessity of applying an equivalent approach to the proper description of immobilized cell catalysis, since oxygen supply should definitely be a critical step in such a three-phase heterogeneous reaction system. Brief reports on the results have been given before (*7*, *8*) and it is the purpose of this paper to provide an insight into the details of our procedure.

Starting with the theoretical aspects of modeling the system, the experimental methods used to determine single system-parameters are described, and finally a comparison of calculated and experimentally determined activity data in the region of diffusional transport control is given.

2. Mathematical Modeling of Immobilized Whole Cell Kinetics

2.1. Consideration of the Problem

The starting point of our consideration of the kinetics of heterogeneous phenol degradation is the well-known differential equation for simultaneous diffusion and isothermal reaction in a spherical catalyst (*9*, *10*).

$$D_e[(d^2c/dr^2) + (2dc/rdr)] = v(c) \tag{1}$$

The right-hand side of Eq. (1) consists of the mathematical description of the homogeneous kinetics in the absence of any diffusional limitation. Considering the stochiometry of our reaction, the concentration ranges, and the diffusion rates of phenol and oxygen, it can be shown that the heterogeneous reaction rate is limited only by oxygen concentration, which then must be inserted into Eq. (1). The influence of oxygen concentration on homogeneous phenol degradation has been investigated in our laboratory (*11*) and by others (*12*). The reaction rate is zero order when the oxygen concentration exceeds about 1/6 of air saturation concentration and is of first order in the lower oxygen concentration range. This behavior must be described by approximations, which may be:

(a) Michaelis-Menten kinetics, where

$$v(c) = v_m \cdot c/(K_M + c) \tag{2}$$

and (b) a zero-order reaction, where

$$v(c) = k_v \tag{3}$$

Solutions of Eqs. (1) and (3) with the boundary conditions

$$r = r_e \qquad c = 0 \qquad dc/dr = 0 \tag{4}$$

$$r = R \qquad c = c_b \tag{5}$$

have been given by Krasuk and Smith (*13*)

$$3/\phi^2 = 2(r_e/R)^3 - 3(r_e/R)^2 + 1 \tag{6}$$

and by Moo-Young and Kobayashi (*14*)

$$\eta = 1 - \{0.5 + \cos[(h + 4\pi)/3]\}^3 \qquad h = \cos^{-1}[6/\phi^2) - 1] \tag{7}$$

$$\eta = 1 - (r_e/R)^3 \tag{8}$$

$$\phi = R(k_v/2D_e \cdot c_b)^{1/2} \tag{9}$$

Catalyst efficiency (η) and Thiele modulus (ϕ) are dimensionless numbers that are widely used in heterogeneous chemical reaction analysis (*9, 10, 15*). η is the ratio of the heterogeneous reaction rate to a reaction rate without diffusional or transport limitations under the same conditions.

It must be mentioned here that we use ϕ as a single abbreviation for Thiele moduli that are differently defined for zero- and first-order and Michaelis-Menten reactions, but its formulae are derived from a generalized definition of ϕ, which has been given by Bischoff (*15*).

Looking at a graphical plot of oxygen concentration between gas phase and catalyst (Fig. 1) we see that substrate concentration on the surface is not identical with substrate concentration in the bulk liquid phase, and therefore that Eqs. (6) and (7) are only approximations for the special case of negligible mass transfer resistance between liquid and solid phase. This approximation is not valid in the case of highly active catalysts and in the case of a microcapsule in which active core and liquid phase are separated by a permeable wall.

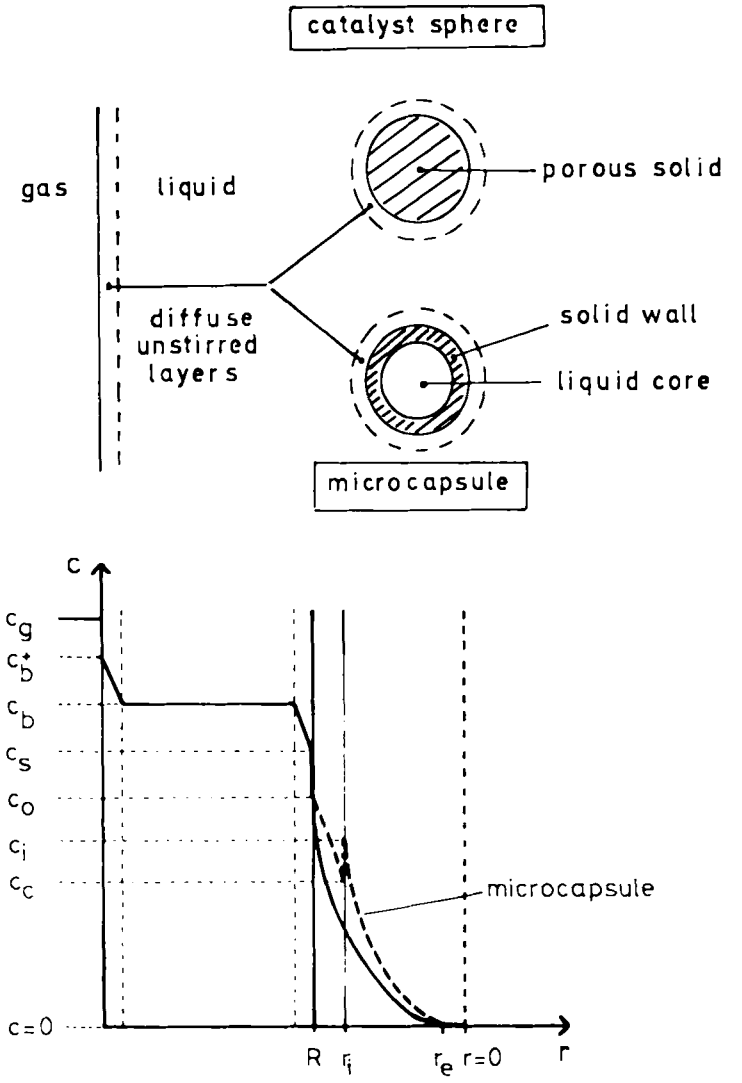

FIG. 1. Schematic drawing of a substrate concentration curve from the gas phase to a catalyst sphere. The special case of a microcapsule is indicated by a thick broken line.

In the following section we derive an equation for a zero-order reaction in a catalyst that includes terms for external mass transfer resistances. We also take into consideration that partition coefficients deviating from unity may arise at the liquid–solid phase boundary, depending on the chemical structure of solid phase and substrate and assuming the catalyst to be a homogeneous phase.

In a later section we apply the method of Na and Na (*16–18*) to solve Eq. (1) for Michaelis-Menten kinetics with consideration of external mass transfer.

2.2. Derivation of an Expanded Equation for Heterogeneous Zero-Order Reaction

External mass transfer resistances taken into consideration here are mass transfer

(a) from gas to liquid phase
(b) from liquid to solid phase
(c) through a permeable wall

Oxygen transfer from air to water may be written:

$$v_F = -(1/V_F)(dN/dt) = k_1a(c^*_b - c_b) \tag{10}$$

Oxygen transfer from bulk liquid to catalyst surface is expressed by Eq. (11)

$$v_F = k_s(c_b - c_s)\, S_c/V_F \tag{11}$$

and diffusion through the wall of a microcapsule is described in Eqs. (12) and (13)

$$v_F = (D_{ew}/V_F)\int_{r_i}^{R}\int_{c_c}^{c_o} 4\pi r^2 (dc/dr) \tag{12}$$

and after integration

$$v_F = 3D_{ew}\, Br_i\,[(c_o - c_c)/R^2(R - r_i)] \tag{13}$$

where

$$B = V_c/V_F = v_F/v_c \tag{14}$$

Introducing the partition coefficients

$$k_{po} = c_o/c_s \tag{15}$$

and

$$k_{pi} = c_c/c_i \tag{16}$$

a combined Eq. (17) can be formulated instead of Eqs. (10) to (14) by eliminating the intermediate concentrations.

$$v_F = 1/\{[R(R - r_i)/D_{ew}k_{po}r_i] + (3B/Rk_1a) + (1/k_s)\}\,[c^*_b - c_i(k_{pi}/k_{po})]\,(3B/R) \tag{17}$$

Equation (17) may be shortened by introducing an overall mass transfer coefficient β.

$$\beta = 1/\{[R(R - r_i)/D_{ew}k_{po}r_i] + (3B/Rk_1a) + (1/k_s)\} \tag{18}$$

Under stationary conditions, mass consumption by reaction is equivalent to mass transfer to and mass transport into the catalyst particle.

$$v_c = (1/V_c)(dN/dt) = D_e(dc/dr)_{r_i}(3/R) = \beta\,[c^*_b - c_i(k_{pi}/k_{po})]\,(3/R) \tag{19}$$

Instead of Eq. (5) we get new boundary conditions from Eq. (19). For a microcapsule:

$$r = r_i\ ,\ c = c_i = (k_{po}/k_{pi})\ [c_b^+ - (D_e/\beta)\ (dc/dr)_{r_i}] \tag{20}$$

For a spherical particle: $c_i = c_o\ ,\ k_{pi} = 1$

$$r = R,\ c = c_o = k_{po}\ [c_b^+ - (D_e/\beta)\ (dc/dr)_R] \tag{21}$$

Integration of Eq. (1) with the boundary conditions (4) and (20) leads to an equation describing catalyst efficiency η as a function of Biot number Bi, Thiele modulus ϕ, and partition coefficients:

$$\eta = 1 - (\{1/[1 - (k_{po}/k_{pi}Bi)]\}\ \{0.5 + \cos[(h + 4\pi)/3]\})^3$$

$$h = \cos^{-1}\ (1 - [1 - (k_{po}/k_{pi}\mathrm{Bi})]^2\ \{(k_{po}/k_{pi})\ [(4/\mathrm{Bi} - 6/\phi^2)] + 2\}) \tag{22}$$

$$\mathrm{Bi} = \beta \cdot R/D_e \tag{23}$$

A detailed derivation of Eq. (22) is given in the appendix. For the case when $k_{po}/k_{pi} = 1$ and $1/\mathrm{Bi} = 0$, Eq. (22) is identical with Eq. (7). It must be noticed that Eq. (22) is only one of three possible solutions of a cubic equation, but it will solve most of the existing practical cases.

2.3. Heterogeneous Michaelis-Menten Kinetics with External Mass Transfer

Equation (1) for Michaelis-Menten kinetics must be solved numerically, which may be done by several methods. We have used the procedure of Na and Na (*16–18*), which is very simple.

A dimensionless form of Eq. (1) for enzyme kinetic may be formulated by substituting

$$c/c_b^+ = y \tag{24}$$

$$r/R = x \tag{25}$$

$$(d^2y/dx^2) + (2dy/xdx) = 2\beta_0 y/(\beta_1 + \beta_2 y + \beta_3 y^2) \tag{26}$$

β_3 is a term for the inhibiting action of substrate or product (*14*).

$$\beta_0 = R^2 v_m/2D_e K_M \tag{27}$$

$$\beta_1 = 1 \tag{28}$$

$$\beta_2 = c_b^+/K_M \tag{29}$$

The boundary conditions for the integration of Eq. (26) are:

$$x = 1\ ,\ y = y_1 = k_{po}/k_{pi}\ [1 - (1/\mathrm{Bi})\ (dy/dx)_1]$$
[dimensionless form of Eq. (20)] (30)

$$x = 0\ ,\ y = y_0\ ,\ dy/dx = 0 \tag{31}$$

Contrary to the zero-order reaction case, the oxygen concentration in the center of particle differs from zero. An ordinate transformation

$$y = A \cdot y^{+}\dagger \tag{32}$$

of Eq. (26) gives Eq. (33), which is independent of A

$$(d^2y^{+}/dx^2) + (2dy^{+}/xdx) = 2\beta_o y^{+}/(\beta_1 + \beta_2^{+} y^{+} + \beta_3^{+} y^{+2}) \tag{33}$$

$$\beta_2^{+} = A \cdot \beta_2 \tag{34}$$

$$\beta_3^{+} = A^2\, \beta_3 \tag{35}$$

Integration of Eq. (33) with an initial-value method such as that of Runge-Kutta leads to values for y_1^{+} and $(dy^{+}/dx)_1$. Integration is started with $y_o^{+} = 1$ and $(dy^{+}/dx)_o = 0$. Then the transformation parameter A is calculated with Eq. (36) derived from Eqs. (30) and (32).

$$A = [(1/\mathrm{Bi})\ (d_y^{+}/dx)_1 + (k_{pi}/k_{po})\ y_1^{+}]^{-1} \tag{36}$$

Retransformation with A leads to the values for y_1 and $(dy/dx)_1$, which, however, belong to a new parameter value $\beta_2 = \beta_2^{+}/A$ and not to the initially introduced value β_2^{+}.

Catalyst efficiency η is the ratio of heterogeneous reaction rate, expressed as rate of diffusion into the catalyst to the rate of unhindered homogeneous reaction.

$$\eta = D_e(dc/dr)_R\, 4\ \pi R^2/(4/3)\ \pi\ R^3\ [v_m\ c_b^{+}/(K_M + c_b^{+})] \tag{37}$$

$$\eta = 3(dy/dx)_1\ (1 + \beta_2)/2\beta_o \tag{38}$$

or

$$\eta = 3(dy/dx)_1\ [(\beta_1 + \beta_2 + \beta_3)/2\beta_o] \tag{39}$$

η may be correlated with ϕ by using a general formula of Bischoff (*15*) which, for the case of $\beta_3 = 0$, leads to

$$\phi = \beta_0^{0.5}\ [\beta_2/(1 + \beta_2)]\ [\beta_2 - \ln(1 + \beta_2)]^{-0.5} \tag{40}$$

Relations for the case that $\beta_3 \neq 0$ have been given by Moo-Young and Kobayashi (*14*).

2.4. Summary

Equation (22) allows the calculation of catalyst efficiency for zero-order kinetics when certain parameter values are known. Thus, k_v is calculated from the amount of immobilized microorganisms per catalyst volume X, the activity of free suspended cells Q, and the activity yield after immobilization Y. Y results from a comparison of the reaction rate of immobilized cells at $\eta = 1$ and the reaction rate of free suspended cells.

$$k_v = Q \cdot Y \cdot X \tag{41}$$

†In this context, A does not yet represent an area; in accordance with the original literature (*16*), it designates the transformation parameter.

D_e, D_{ew}, and k_p values must be measured in diffusion experiments. The value of ϕ is then calculated from Eq. (9), and k_s can be roughly estimated from empirical values. One substrate concentration must be measured. If the concentration in the bulk liquid is known, $k_l a$ is not needed. Otherwise $k_l a$ must be measured (for example, with the sulfite method) since it is very difficult to calculate.

The reaction rate in reactors with stationary conditions is calculated from η with Eq. (42).

$$v_F = k_v \, \eta \, (V_c / V_F) \, (r_i / R)^3 \tag{42}$$

For the calculation of first-order kinetics† in the same manner, we give here the Aris solution (*10*), which we have extended with respect of partition coefficients:

$$1/\eta = (k_{pi}/k_{po}) \, (\phi^2/3) \, ((1/\mathrm{Bi}) + \{1/[(\phi/\tanh \phi) - 1]\}) \tag{43}$$

Numerical integration using the method of Na and Na allows only an indirect calculation of catalyst efficiency. In practical cases, when definite kinetic parameter values have to be considered, the initially used parameter value β_2^* is altered during the integration method by the transformation procedure. Repeated integrations with variations of the parameters β_0 and β_2^* lead to a number of η, β_0 and β_2 values. The corresponding ϕ values are calculated from Eq. (40) and a series of well distributed η and ϕ pairs may serve as a basis for interpolation by a graphical plot of η as a function of ϕ at constant Bi and *kp*. Then in a practical case, ϕ is calculated from Eq. (40) with experimentally determined β_i values, and the corresponding η can be read off from the graphical plot.

3. Experimental Procedures for Parameter Determination

3.1. Reaction Kinetics

3.1.1. Phenol degradation rate. The kinetics of immobilized and free suspended cells were studied in a well-stirred batch-reactor system, as schematically shown in Fig. 2. Polyethylene-flasks (500 mL) were equipped with a hollow glass tube with a four-branch rectangular bottom device. Pressurized air was supplied through the glass core and was frequently dispersed into the fluid at the bottom of the reactor, at the same time providing the momentum for rotational fluid stirring. In a typical experiment with immobilized cells, 0.5 g of catalyst particles were suspended in 300 mL of a 3×10^{-3} *M* phenol solution at a pH = 6.7 controlled by 0.1*M* phosphate buffer. The air supply was sufficient to establish a solution concentration of oxygen close to saturation equilibrium.

A minor part of the solution was continuously circulated to a photometric cell where the phenol concentration was recorded at $\lambda = 270$ nm.

†$\phi = R(k_v/D_e)^{0.5}$; $v_F = k_v \, \eta c_b \, (V_c/V_F) \, (r_i/R)^3$

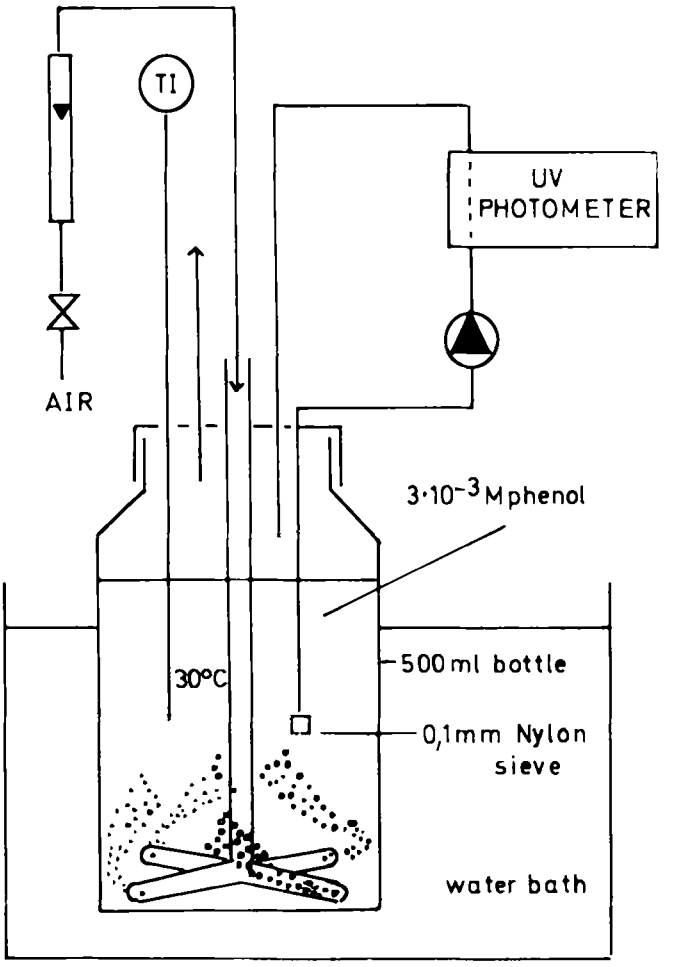

FIG. 2. Experimental device for kinetic measurements. The phenol concentration in the bubble-stirred batch reactor was continuously measured at 270 nm and recorded.

A linear, zero-order plot was obtained for phenol consumption from which the reaction rate could be calculated as follows:

$$v_{Ph} = -dc_{PH}/dt = -dE/d\epsilon dt \qquad (44)$$

An assay of the kinetics of free suspended cells was similarly carried out with about 0.1–0.2 g wet cells.

3.1.2. Oxygen demand. Calculation of catalytic efficiency requires a knowledge of the quantitative value of molar oxygen demand per mole of degraded phenol, since there is evidence from the literature that the simple stoichiometric value of 7 mol O_2/ mol phenol for complete conversion to CO_2 and H_2O could not be used. Oxygen respiration of free *Candida tropicalis* cells was measured with a "Gilson Differential Respirometer." Oxygen respiration of immobilized cells was measured in a fixed-bed reactor with an oxygen-

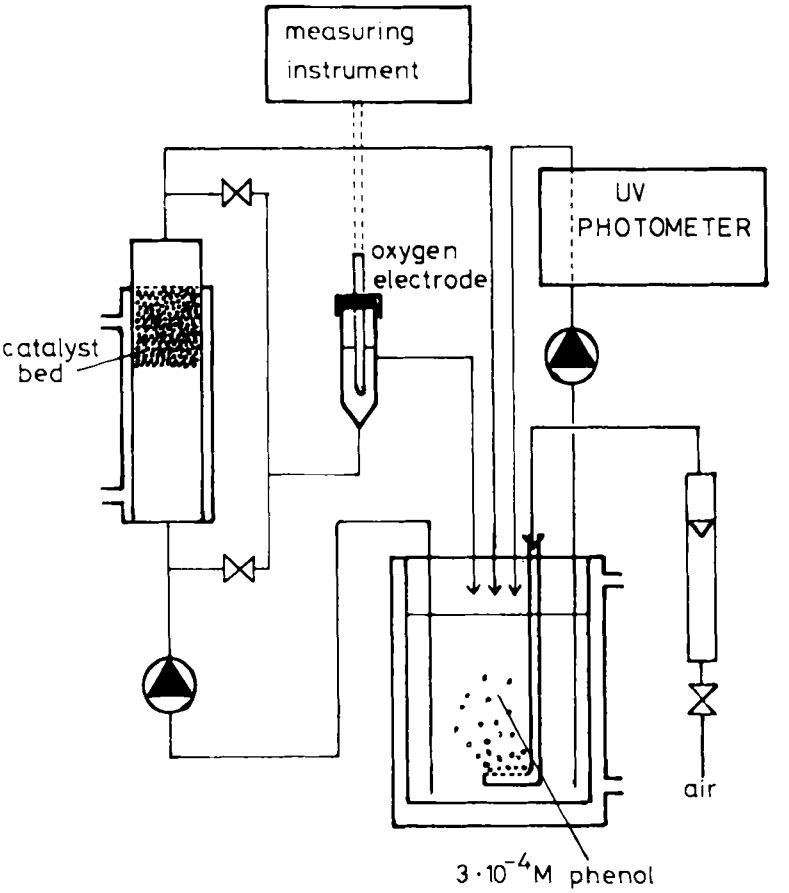

FIG. 3. Estimation of oxygen demand for microbial phenol degradation by simultaneous measurement of oxygen and phenol consumption in a catalyst bed.

sensing electrode device at both ends of the reactor. At a given fluid velocity the oxygen consumption could simply be calculated from the inlet/outlet oxygen concentration difference and then be corrected to the simultaneously recorded phenol consumption. The instrumental setup is shown in Fig. 3.

3.2. Mass Transport and Partition Parameters

3.2.1. Effective diffusion coefficient and permeability coefficient. An experimental device, as shown in Fig. 4, was used for the determination of effective diffusion coefficients D_e in the polymer matrix and for the phenol partition coefficient k_p between the aqueous solution and the catalyst.

Crosslinked polymer discs of 5 cm in diameter and 2-4 mm in thickness were prepared and placed between two metal parts to obtain a two chamber system. The upper chamber was filled with 100 mL of a $10^{-2}M$ phenol solution, connected to an additional reservoir vessel of 300 mL with a circulation pump to maintain practically constant phenol concentration on one side of the membrane. The lower chamber initially contained 5% NaCl solution and the

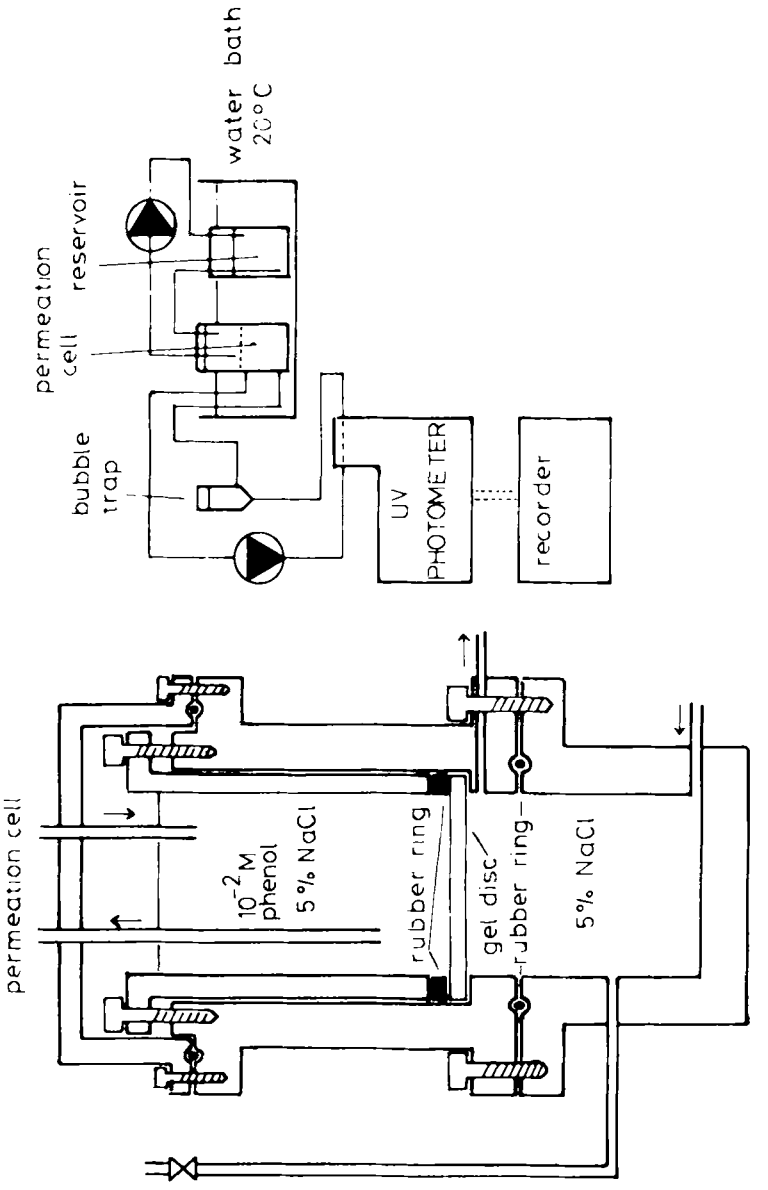

FIG. 4. **Permeation cell for the measurement of phenol diffusion and permeation through a disc of the catalyst carrier. The full arrangement is shown on the right side.**

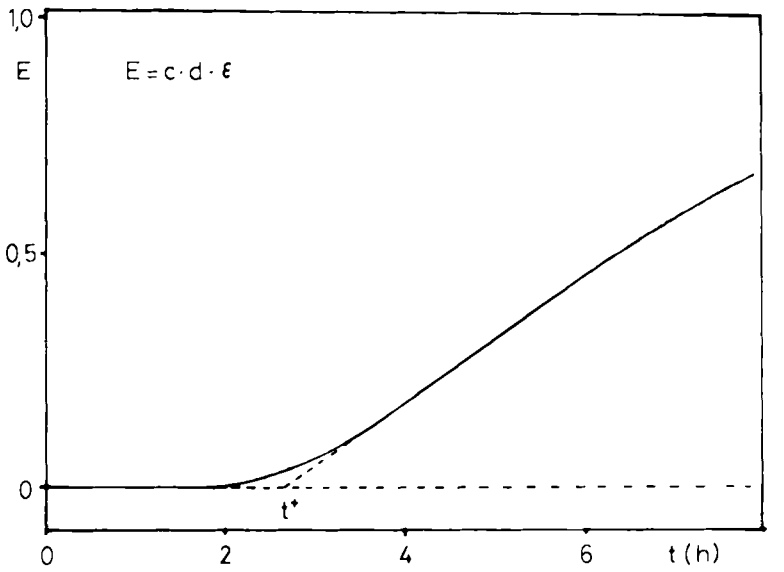

FIG. 5. Recorder trace of the phenol concentration in the lower chamber of the permeation cell.

phenol concentration as a function of time was continuously recorded by circulation through a photometer cell. A schematic drawing of a typical recording is shown in Fig. 5.

The time lag t^+ is used to calculate the diffusion coefficient D_e, while k_p can be obtained from the slope of Fig. 5, which represents the product $(k_p \times D_e)$ which may be designated as permeability coefficient P.

$$D_e = d^2/6t^+ \text{ (ref. 19)} \tag{45}$$

$$k_p D_e = (dc/dt)\,[V/A(dc/dx)] = (dc/dt)\,(Vd/A\Delta c) \tag{46}$$

d = thickness of membrane; A = area of diffusion; V = volume of lower chamber; Δc = concentration difference $\approx$ constant $\approx 10^{-2}M$.

3.2.2. Mass transfer coefficients k_s and $k_L \cdot a$. Empirical correlations for the calculation of k_s have been discussed by Satterfield (*9*). Typical examples are

$$k_s d_p/D_o = 0.997 N_{Pe}^{1/3}$$

$$\text{valid for } N_{Pe} \geqslant 1.000 \tag{47}$$

$$(k_s d_p/D_o)^2 = 4.0 + 1.21 N_{Pe}^{2/3}$$

$$\text{valid for } N_{Pe} \leqslant 10.000 \tag{48}$$

where

$$N_{Pe} = d_p U/D_o \tag{49}$$

N_{Pe} = Pelect number; k_s = mass transfer coefficient liquid/solid (cm/s);

d_p = diameter of particle (cm); D_o = diffusion coefficient in the liquid; U = fluid velocity. Since in a fluidized reaction system a value of U is difficult to obtain, in a first approximation the Pelect number for free sedimentation

$$N_{Pe} = \rho d_p^3 \Delta \rho / \mu D_o 18 \tag{50}$$

(where ρ = density of liquid; $\Delta \rho$ = density difference, solid/liquid; μ = viscosity) can be used. Calculations based on Eqs. (47) and (50) showed only a slight variation of k_s with variable particle sizes to be of interest here. The mean value $k_s = 7 \times 10^{-3}$ cm/s was therefore used further on. No direct attempt was made for a determination of ($k_L \cdot$ a). Under the condition of rather low concentration of catalyst particles in the reaction volume, oxygen concentration in the liquid phase—as confirmed by measurement with an oxygen electrode—was practically identical to saturation concentration. Mass transfer resistance from gas to liquid phase could therefore be neglected. However, the influence of variation of (k_La) values was estimated in some model calculations (Fig. 6b.). Other model calculations show the possible influence of k_s (Fig. 6a) and of the ratio $(r_i/R)^3$ of microcapsules (Fig. 6c).

It can be seen that η is only slightly reduced when k_s falls from values greater 0.1 to 0.007, which is a realistic case. In cases of insufficient stirring, k_s may fall to 0.001, which causes a strong reduction in η. The influence of k_La becomes more important when B, the loading of reactor with catalyst particles, is increased.

Microcapsules have only small catalyst activities when their core volumes, which contain the enzymatic active species, are too small compared to the volume of an overall particle. It is therefore necessary to prepare microcapsules with thin but very stable walls. It should be noted that η in Fig. 6c is only related to the capsule core and not to the overall capsule volume.

3.3. Reincubation of PMAAm Entrapped Candida tropicalis *Cells*

Wet PMAAm beads containing 0.025 g/cm^3 *Candida tropicalis* cells, with 23% alive after immobilization, were rinsed thoroughly for 12 h at 4°C with a 9% sterilized NaCl solution to clean the surface from adsorbed cells. In a number of parallel experiments 0.5 g of the wet PMAAm beads were incubated at 30°C with 100 cm^3 of a nutrient medium and vigorously shaken in sterile 1-L Erlenmeyer flasks.

Five hours later, incubation was stopped and the beads were again rinsed for 12 h with a 0.9% NaCl solution. The activity of all fractions of different catalyst particle radius had risen to about 2×10^{-5} mol/cm^3-h. Then the incubation was again conducted as described above for 50 h. Some samples were removed from the incubation flask after shorter times and washed again thoroughly with 0.9% NaCl solution to eliminate residual nutrient medium and phosphate. Elemental analysis for the phosphorus content of some preparations was carried out to determine whether there is an increased amount of cells. The

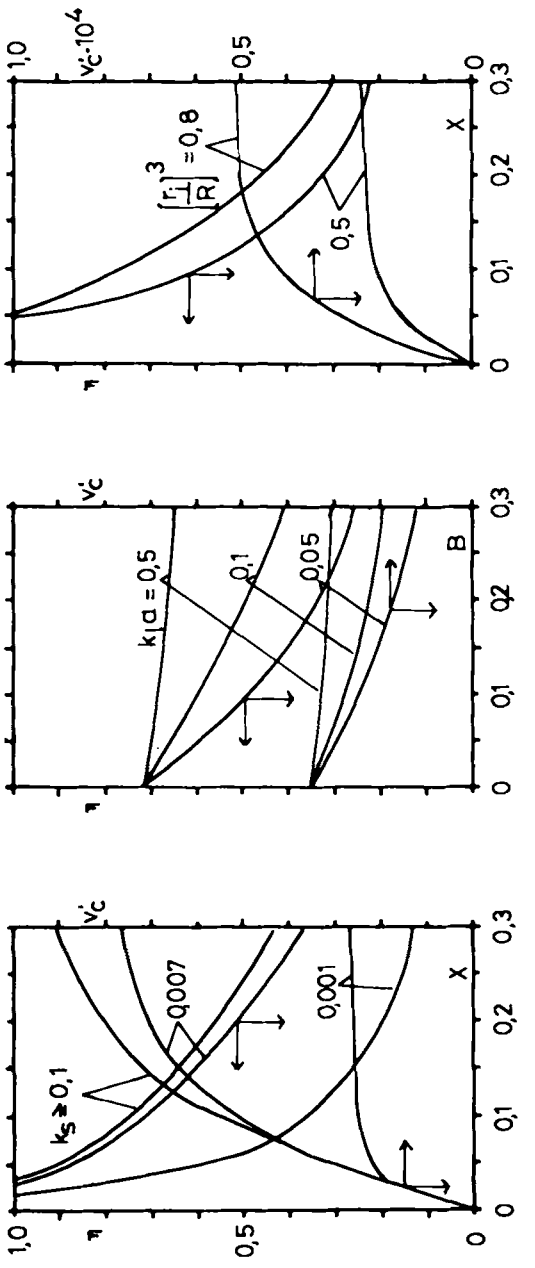

FIG. 6. Model calculations, based on Eq. (22), showing the possible influences of k_s, k_1a, and the active volume of microcapsules on catalyst efficiency and phenol degradation rate.

catalytic activity of the preparations was determined as described previously. The nutrient medium and the salt solution have been used as follows:

Nutrient medium	Salt solution
Phenol, 1g	$ZnSO_4$, 11 g
Yeast extract, 1 g	$MnSO_4 \cdot H_2O$, 6 g
NH_4NO_3, 2 g	$FeSO_4 \cdot 7H_2O$, 1 g
$(NH_4)_2SO_4$, 2 g	$CoSo_4 \cdot 7H_2O$, 0.3 g
KH_2PO_4, 1 g	$CuSO_4 \cdot 5H_2O$, 40 mg
$K_2HPO_4 \cdot 3H_2O$, 2 g	H_3PO_4, 60 mg
$Na_2HPO_4 \cdot 2H_2O$, 1 g	KJ, 1 mg
$MgSO_4 \cdot 7H_2O$, 0.2 g	EDTA, 5 g
KCl, 0.2 g	
Salt solution, 1 mL	
Water	Water
To 1000 mL	To 1000 mL

4. Results and Discussion

4.1. Results of Model Calculations Based on Michaelis-Menten Kinetics

The results of some numerical calculations, using a fourth-order Runge-Kutta integration procedure, are given in Table 1. It can be seen that up to 10 steps may be necessary to obtain a good approximation to a limiting value. On the other hand the critical influence of an inappropriate choice of the parameters β_0 and β_2^+ on the resulting values of β_2, η, and ϕ can be evaluated. In Table 2, given sets of ϕ, Bi, and k_p values as well as catalytic efficiencies η for different reaction kinetics, namely zero-order Michaelis-Menten kinetics and first-order kinetics for the limiting substrate concentration, are presented.

At higher substrate concentrations, i.e., $c_0/K_m > 2$, the values for MM-kinetics show only minor differences compared to the zero-order case. Under these conditions the numerical integration procedure can easily be substituted without loss of accuracy by the analytical solution available for zero-order. Care however must be observed at low values of $Bi < 4$ and high values of k_{po}/k_{pi} since the analytical solution may not be possible owing to extreme cosine arguments.

An increase in k_{po}, such as might be achieved by an appropriate modification of the polymer matrix to enhance substrate sorption, certainly has a larger effect on η in a first-order reaction compared to the effect in a zero-order reaction. This then would correspondingly apply for cases of lower substrate concentration $c_b/K_M \leqslant 1$ in Michaelis-Menten kinetics.

TABLE 1
Initial Parameter Values and Results of Numerical Integrations with the Method of Na and Na[a]

$\beta_0 \times 2$	β_2^*	Bi	N^b	β_2	η	ϕ
400	1×10^{-5}	5	5	22.708	0.504	3.064
400	1×10^{-5}	5	10	24.856	0.538	2.925
400	1×10^{-5}	5	30	23.807	0.523	2.991
400	1×10^{-5}	5	50	23.650	0.521	3.001
8000	1×10^{-17}	4	5	94	0.121	6.59
8000	1×10^{-17}	4	10	771	0.677	2.29
8000	1×10^{-17}	4	20	1120	0.830	1.89
400	1×10^{-3}	12	10	40.902	0.833	2.264
400	1×10^{-4}	12	10	28.293	0.713	2.737
400	3×10^{-7}	12	10	4.342	0.240	7.039
400	1×10^{-7}	5	10	7.374	0.221	5.436
400	1×10^{-7}	5	10	3.877	0.136	7.425
400	1×10^{-6}	5	10	12.508	0.331	4.161
400	1×10^{-4}	5	10	39.008	0.706	2.32
100	5×10^{-2}	5	10	23.595	0.984	1.502
100	6×10^{-3}	12	10	3.956	0.522	3.678
100	2×10^{-3}	12	10	2.187	0.389	4.786
200	1×10^{-3}	12	10	10.497	0.606	3.217

[a]Calculations were done with a Hewlett Packard HP 67 calculator. ($k_p = 1$)
[b]N = number of integration steps.

4.2. Oxygen Respiration

Photometric determination of phenol concentration as function of time of free suspended cells only gives the specific rate of phenol consumption, Q_{Ph}, of *Candida tropicalis*, from which the rate constant

$$k_v' = Q_{Ph}X \tag{51}$$

where k_v' is the rate constant for phenol disappearance and X is the cell concentration, can be calculated. Since oxygen is the rate-controlling cosubstrate, the rate constant for oxygen consumption

$$k_v = Q_{ox}X = k_v'(Q_{ox}/Q_{Ph}) \tag{52}$$

is needed.

The ratio Q_{ox}/Q_{Ph} is equal to the number of moles of O_2 actually consumed to convert 1 mole of phenol to final products. Neujahr et al. (*20*) reported $Q_{ox}/Q_{Ph} = 3.5$ from Warburg experiments, while a value higher than 4 was observed by Nei et al. (*21*). Calculations based on a value of 3.5, however, gave much higher catalyst efficiency values than were observed by us experimentally.

An example of an instationary respiration experiment in the Gilson

TABLE 2
Influence of Partition Coefficient and Reaction Order on Catalyst efficiency

				Catalyst efficiency		
k_{po}	Bi	ϕ	c_b/K_M	Zero-order	Michaelis-Menten	First-order[a]
1.0	12	7.039	4.342	0.237	0.240	0.243
1.0	12	4.786	2.187	0.397	0.389	0.377
1.0	12	3.678	3.956	0.539	0.522	0.486
1.0	12	3.217	10.497	0.620	0.606	0.545
1.0	12	2.737	28.293	0.724	0.713	0.615
1.0	12	2.264	40.902	0.845	0.823	0.693
0.8	12	20.0	—	0.041	—	0.055
0.8	12	9.130	2.446	0.153	0.152	0.140
0.8	12	6.653	4.887	0.242	0.235	0.208
0.8	12	3.307	19.574	0.560	0.544	0.426
0.8	12	2.067	48.869	0.848	0.829	0.582
2.0	12	20.0	—	0.043	—	0.110
2.0	12	10.0	—	0.154	—	0.309
2.0	12	5.0	—	0.455	—	0.720
2.0	12	2.0	—	[b]	—	1.479

[a] η was calculated according to Aris (*10*).
[b] In this case, the $\cos^{-1}$ argument of Eq. (22) allowed no calculation.

Respirometer is shown in Fig. 7. A curve (1) showing the molar consumption ratio Q_{ox}/Q_{Ph} as function of time is combined with a second curve (2), showing the difference of oxygen consumption and CO_2 production; thus, from these two curves the molar production of CO_2 per mole phenol can be obtained as well. Parabolic extrapolation of curve (1) to $t = \infty$ gives a limiting value of about $Q_{ox}/Q_{Ph} = 5$–5.5. Considering the contribution of endogenic respiration, a value of 4–4.5 is obtained.

In the second approach, a stationary value of Q_{ox}/Q_{Ph} was obtained using a fixed-bed reactor in a continuous mode. The data of these experiments with two different catalyst preparations are summarized in Table 3. The average value of $Q_{ox}/Q_{Ph} = k_v/k'_v = 4.67$, which includes the actual contribution of endogenic respiration, confirms the former results. Throughout the following calculations, the value $Q_{ox}/Q_{Ph} = 4.5$ was used. No further attempt was made in this study to develop a more detailed understanding of the reaction pathway during phenol degradation (*21*).

4.3. Diffusion and Partition

The diffusion experiments were first carried out on polymer network preparations with no entrapped cells. In Fig. 8 the results of the phenol diffusion and permeation studies are shown in a graph of D_e and P,

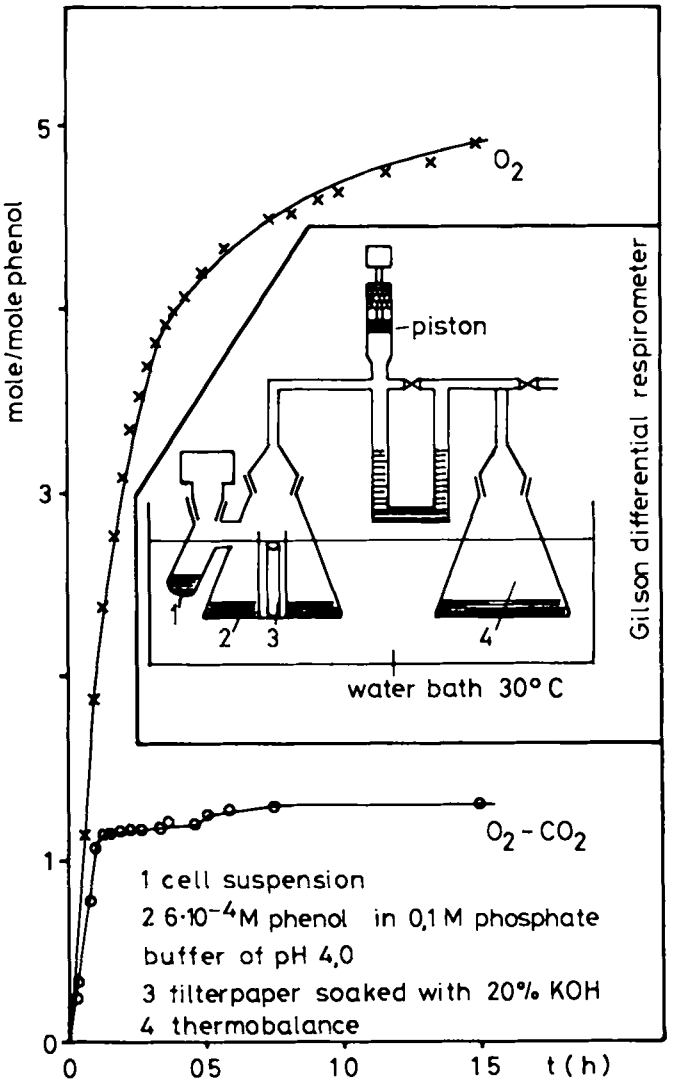

FIG. 7. Volumetric measurement of oxygen demand for the microbial phenol oxidation with a Gilson differential respirometer.

TABLE 3
Results of the Measurement of the Oxygen Demand Related to Phenol in the Fixed-Bed Reactor of Fig. 3

Parameters	Catalyst 1		Catalyst 2	
$\mathring{v}$ (m^3/h)[a]	0.092	0.085	0.091	0.086
$\Delta c_{ox} \times 10^5$ (mol/L)	3.29	2.58	6.82	6.58
$\mathring{v}\Delta c_{ox} \times 10^3$ (mol/L)	3.01	2.19	6.23	5.69
$\Delta c_{ph}\ V/t \times 10^3$ (mol/h)	0.634	0.481	1.28	1.28
$\mathring{v}\Delta c_{ox}/(\Delta c_{ph}\ V/t) = Q_{ox}/Q_{ph}$	4.74	4.55	4.86	4.44

[a]Quantity of liquid passing the fixed bed catalyst per hour.

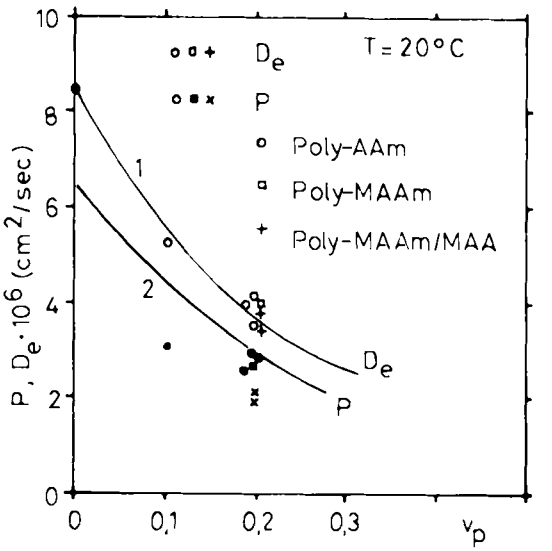

FIG. 8. Influence of polymer volume fraction on phenol diffusion coefficient and permeability in various polymer networks.

respectively, as functions of polymer concentration, where the different symbols represent different chemical network types. The curves (1) and (2) are represented by the equations

$$D_e/D_o = \exp - 4v_p \tag{53}$$

where v_p is the volume fraction of polymer in the network, and

$$P = k_p D_e \tag{54}$$

where the value $D_o = 8.5 \times 10^{-6}$ cm^2/s has been taken from the literature (*22*). Since the data obtained by White and Dorion (*23*) show that the factor 4 in the exponent of Eq. (53) is the limiting value for small molecules, we felt justified in also applying Eq. (53) to oxygen diffusion. The ratio D_e/P gives a partition coefficient of $k_p = 0.8$ that seems to reflect more accurately the ratio of pore volume to total volume than any specific interaction mechanism. Under these circumstances, the value $k_p = 0.8$ would be assumed to hold for oxygen as well.

Substrate diffusion becomes more restricted if immobilized cell preparations are considered. In these sets of experiments, different cell concentrations have been entrapped in polymer networks at constant polymer concentration ($v_p = 0.2$ based on the cell-free volume). Despite some scattering, the resuls for the diffusion coefficient may be correlated by Eq. (55):

$$D_e/D_o = (1 - X)^2 \exp - 4vp \tag{55}$$

For PAAm and PMAAm networks, the value $k_p = 0.8$ can again be obtained from the composition of diffusion and permeation (see Fig. 9). However, some care should be observed in generalizing such results too early since permeation data obtained with a slightly ionic network (PMAAm + acrylic acid comonomer) require a definitely lower value of k_p (see Fig. 10).

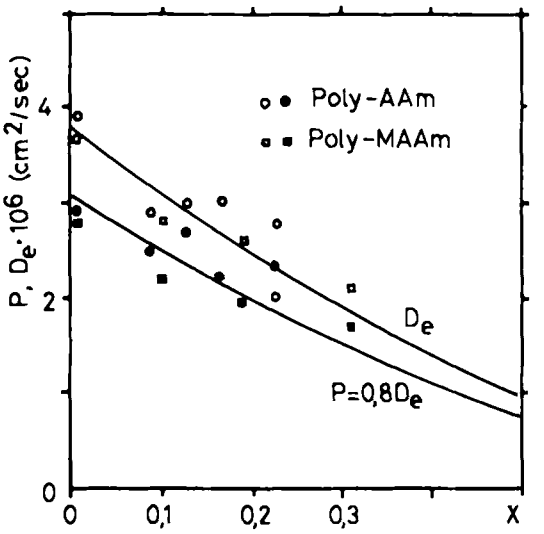

FIG. 9. Influence of cell concentration on permeability of nonionic polymer networks ($\nu_p = 0.2$).

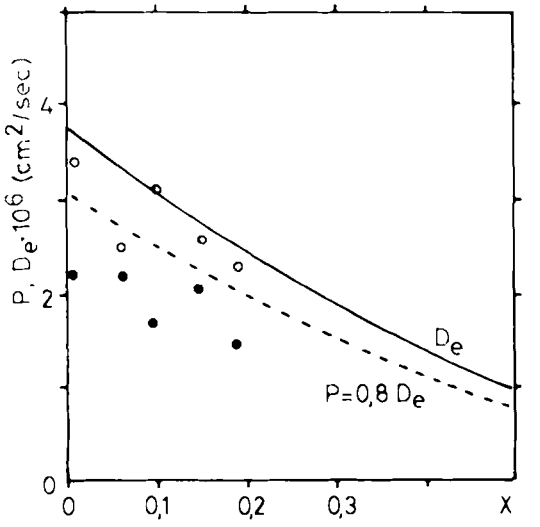

FIG. 10. Reduced permeability of phenol in an anionic polymer network (MAAm/MAA copolymer, $\nu_p = 0.2$).

4.4. *Catalytic Efficiency of* Candida tropicalis *in PAAm Networks*

Experimental results on the reaction rate for phenol degradation by PAAm-entrapped cells of *Candida tropicalis* are summarized in Fig. 11, and may be compared with calculations based on Eq. (22) of the mathematical model (see section 2.2). The ordinate shows the phenol degradation rate ν_c' while different cell concentrations X are given on the abscissa. The curves represent studies

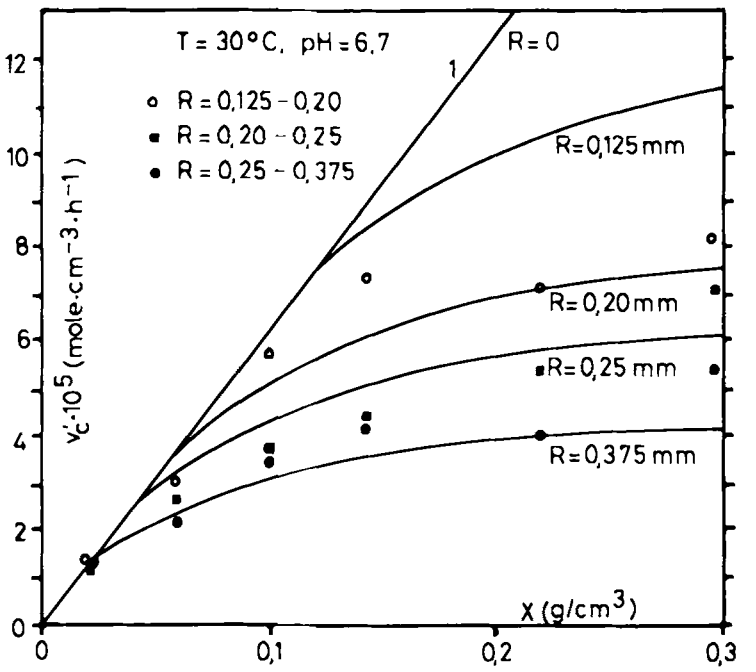

FIG. 11. Comparison of phenol degradation rates of PAAm entrapped *Candida tropicalis* as function of particle size and cell content in the catalyst particle with calculations based on Eq. (22).

with catalyst particles of different diameter, and the experimental data symbols represent results obtained with three different particle size regions.

The straight line denoted 1 represents those activity values that can or might be obtained if all surviving immobilized cells contributed 100% activity. This would of course be equivalent to the kinetics of freely suspended cells or to the limiting value of particle size $R = 0$.

The parameter values used in calculations based on Eq. (22) are given in Table 4.

TABLE 4
Parameter Data Used for Model Calculations

$v_c = Q_{ox} X Y$
$Q_{ox} = 2.7 \times 10^3$ {mol/[g(wet)h]} $= 4.5 Q_{ph}$
$v_c = 4.5 v_c'$
$Y =$ activity yield after immobilization $= 0.9$
$kp_o = 0.8$
$k_s = 7 \times 10^{-3}$ cm/s
$c_b = c_b^* = 2.3 \times 10^{-7}$ mol/cm^3 (ref. *24*)
$D_o = 2.8 \times 10^{-5}$ cm^2/s (ref. *24*)
$v_p = 0.1$
$D_e = D_o (1 - x)^2 \exp(-4 v_p)$

The model calculations clearly show increasing diffusional limitation with increasing particle size from $R = 0.125$ mm to $R = 0.375$ mm. Deviation from line 1 therefore occurs earlier as the catalyst particle size increases, i.e., between $X \approx 0.03$ (for $R = 0.375$) and $X \approx 0.12$ (for $R = 0.125$ mm).

The experimental values of $X = 0.03$ for all particle sizes represent values in the reaction controlled regime (i.e., $\eta = 1$), while increasing cell concentration leads to a differentiation based on diffusional limitations.

The results for the 0.125–0.20 fraction and for the 0.25–0.375 fraction are in especially good agreement with the computed values.

This seems to be an indication for the applicability of the mathematical model and for the accuracy of the experimentally determined parameters to be used in these calculations.

The data for the 0.20–0.25 fraction for several intermediate X values are definitely smaller than theoretically expected. This and the scattering of the experimental data are presumably caused by difficulties in getting an exact weight of the wet catalyst. Values of the activities for all preparations at $X = 0.06$ and 0.22 that are too low may be related to a somewhat higher toxic inactivation during immobilization, thus requiring values of $Y < 0.9$ in the calculation.

4.5. Activity of PMAAm Preparations and Reincubation

As reported in the preceding paper, entrapment in PMAAm results in a generally higher loss of enzymatic activity compared to PAAm, and values of $Y \approx 0.3$ (as compared to $Y = 0.9$ for PAAm) are quite typical.

Although the mechanical properties of the PMAAm beads are superior to those formed by PAAm, only significantly lower catalytic activities are observed after immobilization.

As reported earlier (*7*), however, living immobilized cell systems can be activated by incubation with required nutrients. Based on "secondary" cell growth in the polymeric matrix, the number of immobilized and active cells can be drastically increased, accompanied by a related increase in catalytic activity.

The increase in reaction rate for phenol degradation as a function of incubation time is demonstrated in Fig. 12.

Based on elemental analysis of the phosphorus content of immobilized cell preparations during this incubation procedure, the average cell concentration can be estimated to rise from an initial value of 0.025 (with residual activity of 20%) to a value of $X = 0.08$ (after 27 h) and $X = 0.14$ (after 55 h) where the latter value seems to be a limiting one.

Following the calculated lines in Fig. 11, the limiting maximum value of catalytic activity for a given particle size seems to require cell concentrations above $X = 0.20$. The corresponding approach to a maximum value in Fig. 11 at a much lower value of X seems to be indication for an inhomogeneous cell distribution in the catalytic particle, caused by preferential cell growth in the outer shell and diffusion-controlled growth conditions.

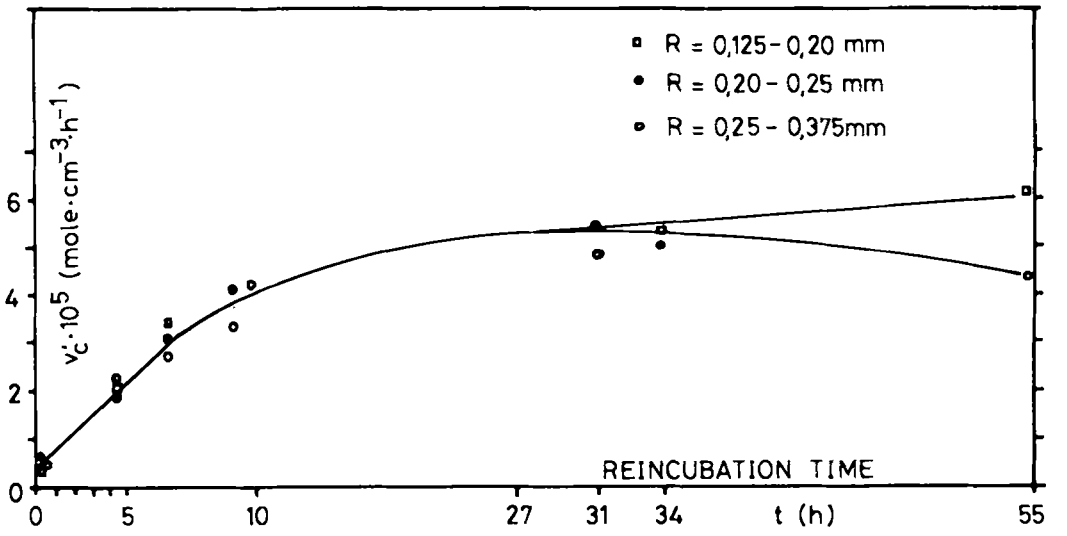

FIG. 12. Phenol degradation rate of a catalyst preparation as function of reincubation time.

Maximum activities of PMAAm preparations after incubation are quite comparable to the maximum activities of PAAm-particles, as can be seen from Table 5, where the slightly lower values of the PMAAm series seems to be caused by the polymer concentration ($v_p = 0.2$ as compared to $v_p = 0.1$ for PAAm).

Using PMAAm-embedded cells, an interesting observation has been made with regard to their stability in the presence of oxygen. Experiments with free suspended cells of *Candida tropicalis* showed a very fast and practically quantitative loss of catalytic activity if the oxygen concentration was higher than air saturated. Thus oxygen could be supplied only in a diluted fashion, as in air.

Phenol degradation experiments with PMAAm-immobilized cells have then been performed in which pure oxygen was supplied at increasing levels.

As shown in Table 6, increasing the oxygen concentration levels in the solution increased the rate of phenol conversion. Diffusion limitation

TABLE 5

Comparison of the Maximum Activity of Polyacrylamide- and Polymethacrylamide Network-Entrapped *Candida tropicalis* Cells

R, mm	v_c (PAAm: $v_p = 0.1$)	v_c (PMAAm: $v_p = 0.2$)[a]	v_c (calculated)[b]
0.125–0.20	8.24×10^5	6.18×10^5	6.6×10^5
0.20–0.25	7.11×10^5	5.42×10^5	5.9×10^5
0.25–0.375	5.36×10^5	5.81×10^5	3.9×10^5

[a]After reincubation with a nutrient medium.
[b]$X = 0.3$ (assumption); $v_p = 0.2$.

TABLE 6
Influence of Oxygen Concentration on the Activity of Polymethacrylamide Network-Entrapped *Candida tropicalis* Cells

c_{ox}, mg/L	v_c ($R = 0.2$–0.25)	v_c (calculated)[a]
7.2	5.32×10^5	4.37–5.46×10^5
20.0	6.96×10^5	6.36–7.23×10^5
36.0	7.67×10^5	7.39–8.08×10^5

[a]With the assumption that $\bar{X} = 0.12$.

obviously results in an intraparticular concentration decay down to a level where cell activity is maintained.

Assuming a cell concentration of $X = 0.12$ (based on the activity level at the usual oxygen concentration level), the increasing reaction rates can be readily simulated by our mathematical model (see Table 6).

Appendix

Derivation of Eq. (22) in section 2.2.

$$d^2c/dr^2 + (2dc/rdr) = k_v/D_e \tag{A.1}$$

$$c/c_b^+ = y \tag{A.2}$$

$$r/R = x \tag{A.3}$$

$$d^2y/dx^2 + (2dy/xdx) = 2\phi^2 \tag{A.4}$$

$$\phi^2 = R^2k_v/2D_ec_b^+ \tag{A.5}$$

The general solution of differential Eq. (A.4) is:

$$y = (1/3)\ \phi^2x^2 - (K_1/x) + K_2 \tag{A.6}$$

where K_1, K_2 are integration constants

$$dy/dx = (2/3)\ \phi^2x + (K_1/x) \tag{A.7}$$

The boundary condition $(dy/dx)_{x_e} = 0$ allows the calculation of K_1

$$K_1 = -(2/3)\ \phi^2x_e^3 \tag{A.8}$$

Introducing the dimensionless form of Eq. (20) from section 2 as a second boundary condition

$$x = 1,\ y = (k_{po}/k_{pi})\ [1 - (1/\mathrm{Bi})\ (dy/dx)_1] \tag{A.9}$$

we get

$$K_2 = (k_{po}/k_{pi})\ [1 - (1/\mathrm{Bi})\ (dy/dx)_1] - (2/3)\ \phi^2x_e^3 - (1/3)\ \phi^2 \tag{A.10}$$

Eqs. (A.8) and (A.10), when inserted into Eq. (A.6), lead to a description of the concentration curve in the catalyst pellet

$$y = (1/3)\ \phi^2 x^2 + (2/3)\ \phi^2\ (x_e^3/x) + (k_{po}/k_{pi})$$
$$[1 - (1/\mathrm{Bi})\ (dy/dx)_1] - (2/3)\ \phi^2 x_e^3 - (1/3)\ \phi^2 \qquad \text{(A.11)}$$

At $x = x_e$, we have $y = 0$, and with the first derivation of Eq. (A.11)

$$(dy/dx)_1 = (2/3)\ \phi^2 - (2/3)\ \phi^2 x_e^3 \qquad \text{(A.12)}$$

we get

$$0 = \phi^2 x_e^2 + (k_{po}/k_{pi})\ \{1 - (1/\mathrm{Bi})$$
$$[(2/3)\ \phi^2 - (2/3)\ \phi^2 x_e^3]\} - (2/3)\ \phi^2 x_e^3 - (1/3)\ \phi^2 \qquad \text{(A.13)}$$

Division by ϕ^2 and simplification leads to Eq. (A.14)

$$0 = (2/3)\ [1 - (k_{po}/k_{pi})\ (1/\mathrm{Bi})]\ x_e^3 - x_e^2 + (2/3)$$
$$(k_{po}/k_{pi})\ (1/\mathrm{Bi}) - (k_{po}/k_{pi})\ (1/\ \phi^2) + (1/3) \qquad \text{(A.14)}$$

This is a cubic equation of the form

$$0 = a_3 x_e^3 + a_2 x_e^2 + a_1 x_e + a_o \qquad \text{(A.15)}$$

with $a_2 = -1$ and $a_1 = 0$. One of the three solutions is (Hewlett Packard HP 67 standard programs):

$$x_e = 2M^{0.5} \cos\ \{(1/3)\ \cos^{-1}\ [N/(-M^3)^{0.5}]\} - a_2/3a_3 \qquad \text{(A.16)}$$

$$M = [3a_1 - (a_2^2/a_3)]/9a_3 = -\ 1/9a_3^2 \qquad \text{(A.17)}$$

$$N = [(9a_2a_1/a_3) - 27a_o - (2a_2^3/a_3^2)]/54a_3 = -\ a_o/2a_3 + 1/27a_3^3 \qquad \text{(A.18)}$$

Introducing Eqs. (A.17) and (A.18) into Eq. (A.16) we get

$$x_e = (2/3a_3)\ \cos\ \{(1/3)\ \cos^{-1}\ [1 - (27/2)a_o a_3^2]\} + 1/3a_3 \qquad \text{(A.19)}$$

$$x_e = (2/3a_3)\ (0.5 + \cos\ \{1/3\ \cos^{-1}\ [1 - (27/2)\ a_o a_3^2]\}) \qquad \text{(A.20)}$$

$$\cos^{-1}\ [1 - (27/2)a_o a_3^2] = h \qquad \text{(A.21)}$$

$$x_e = \{1/[1 - (k_{po}/k_{pi})\ (1/\mathrm{Bi})]\}\ [0.5 + \cos\ (1/3)h] \qquad \text{(A.22)}$$

The value of the catalyst efficiency of a zero-order reaction is identical with the fraction of active catalyst volume

$$\eta = V_a/V_c = (R^3 - r_e^3)/R^3 = 1 - x_e^3 \qquad \text{(A.23)}$$

$$\eta = 1 - (\{1/[1 - (k_{po}/k_{pi})\ (1/\mathrm{Bi})]\}\ \{0.5 + \cos\ [(h + 4\pi)/3]\})^3 \qquad \text{(A.24)}$$

$$h = \cos^{-1}\ (1 - (27/2)\ (4/9)\ [1 - (k_{po}/k_{pi})\ (1/\mathrm{Bi})]^2$$
$$(2/3)\ (k_{po}/k_{pi})\ (1/\mathrm{Bi}) - (k_{po}/k_{pi})\ (1/\phi^2) + (1/3) \qquad \text{(A.25)}$$

$$h = \cos^{-1}\ (1 - [1 - (k_{po}/k_{pi})\ (1/\mathrm{Bi})]^2 \qquad \text{(A.26)}$$
$$\{(k_{po}/k_{pi})\ [(4/\mathrm{Bi}) - (6/\phi^2)] + 2\})$$

The term 4π must be added to h to get calculable cosine arguments in Eq. (A.24).

Acknowledgments

The fruitful cooperation of Professor F. Wagner and his research group as well as the financial support of the BMFT under grant No. BCT 65 is gratefully acknowledged. This paper is drawn in part from the dissertation of Peter Schara at the Technical University of Braunschweig, 1977, "Einschluss von Mikrooorganismen in hydrophile, kovalente Polymernetzwerke—Zum Aufbau und zur Reaktivität von Biokatalysatoren für Mehrphasenreaktionen."

List of Abbreviations and Symbols

- A Area of gel disc in diffusion experiments (cm^2)
- a Area of gas–liquid boundary per unit of fluid volume (cm^2/cm^3)
- B Ratio of particle volume to fluid volume
- Bi Biot number
- c Concentration (mol/cm^3)
- c_b Concentration in the bulk liquid
- c_b^* Saturation concentration of a gaseous substrate in liquid
- c_i Concentration on the inner side of a microcapsule wall
- c_i Concentration at the inner side of a microcapsule wall
- c_o Concentration at the surface of a catalyst particle in the liquid
- c_s Concentration at the surface in equilibrium to c_o
- D_e Effective diffusion coefficient (cm^2/s)
- D_{em} Effective diffusion coefficient in a microcapsule wall
- D_o Diffusion coefficient in a liquid (cm^2/s)
- d_p Diameter of a particle (cm)
- d Thickness of a membrane (cm); length of absorbance in UV spectroscopy (cm)
- E Absorbance
- F Fluid
- k_l Mass transfer coefficient gas–liquid (cm/s)
- k_s Mass transfer coefficient liquid–solid (cm/s)
- k_p Partition coefficient
- k_v Reaction rate constant (mol/cm^3-s)
- K_M Michaelis-Menten constant (mol/cm^3)
- N_{Pe} Peclet number
- N_{Re} Reynolds number
- P Permeability coefficient (cm^2/s)
- Q_{Ox} Oxygen consumption by microorganisms (mol/s-g (wet))
- Q_{Ph} Phenol consumption by microorganisms (mol/s-g (wet))
- R Radius of catalyst particle (cm)
- r_e Radius at which oxygen concentration becomes zero (cm)
- r_i Inner radius of the wall of a microcapsule (cm)
- S_c Surface of the catalyst particle (cm^2)
- t Time (s)
- t^* Time lag (s)
- U Fluid velocity (cm/s)
- V_c Volume of the catalyst particle (cm^3)
- V_F Volume of fluid (cm^3)

v_c Reaction rate per catalyst volume (mol/cm^3-s)
v_F Reaction rate per fluid volume (mol/cm^3-s)
v_m Maximum reaction rate in Michaelis-Menten kinetics
v_p Polymer volume fraction of catalyst particle volume
X Concentration of cell mass [g (wet)/cm^3]
x Dimensionless radius
Y Activity yield after immobilization
y Dimensionless concentration
β Combined mass transfer coefficient (cm/s)
ϵ Absorbance coefficient
η Catalyst efficiency
μ Viscosity [g/(s-cm)
ρ Density (g/cm^3)
θ Thiele modulus

References

1. Klein, J., and Schara, P. (1979), *J. Solid Phase Biochem.* **5,** 61.
2. Kasche, V., Lundquist, H., Bergman, R., and Axén, R. (1971), *Biochem. Biophys. Res. Commun.* **45,** 615.
3. Korus, R., and O'Driscoll, K. F., *Canad. J. Chem. Eng.* **52,** 5 (1974).
4. Vieth, W. R., Venkatasubramanian, K., Constantinides, A., and Davidson, B.(1976), *Appl. Biochem. Bioeng.* **1,** 221.
5. Greenfield, P. F., Kittrell, J. R., and Laurence, R. L. (1976), *Anal. Biochem.* **65,** 109.
6. Buchholz, K., and Reuss, M. (1977), *Chimia* **31,** 27.
7. Klein, J., Hackel, U., Schara, P., Washausen, P., and Wagner, F. (1976), *Abstr. 5th Intern. Ferment. Symp. Berlin,* 295.
8. Klein, J., Hackel, U., Schara, P., Washausen, P., Wagner, F., and Martin, C. K. A. (1978), *Enzyme Eng.* **4,** 339.
9. Satterfield, C. N. (1970), *Mass Transfer in Heterogeneous Catalysis,* Cambridge, Mass.
10. Aris, R. (1975), *The Mathematical Theory of Diffusion and Reaction in Permeable Catalysts,* vol. 1, Clarendon Press, Oxford.
11. Washausen, P. (1975), Diplomarbeit, Institut f. Chemische Technologie der Technischen Universität Braunschweig.
12. Nei, N., Enatsu, T., and Terui, G. (1973), *J. Ferm. Techn.* **51,** 1.
13. Krasuk, J. H., and Smith, J. M. (1965), *Ind. Eng. Chem. Fund.* **4,** 102.
14. Moo-Young, M., and Kobayashi, T. (1972), *Can. J. Chem. Eng.,* **50,** 162.
15. Bischoff, K. B. (1965), *AIChEJ.* **11,** 351.
16. Na, H. S., and Na, T. Y. (1970), *Mathem. Biosci.* **6,** 25.
17. Fink, D. J., Na, T. J., and Schultz, J. S. (1973), *Biotech. Bioeng.* **15,** 879.
18. Wadiak, D. T., and Carbonell, R. G. (1975), *Biotech. Bioeng.* **17,** 1761.
19. Daynes, H. A. (1920), *Proc. Roy. Soc. (London)* **A97,** 286.
20. Neujahr, H. J., Lindsjö, S., and Varga, J. M. (1974), *Antonie van Leuwenhoek* **40,** 209.
21. Klein, J., and Hackel, U. (1979), *ACS Symp. Series* **106,** 101.
22. Erdös, E., and Nyvld, J. A. (1958), *Collect. Czechoslov. Chem. Comm.* **23,** 579.
23. White, M. L., and Dorion, G. H. (1961), *J. Polym. Sci.* **55,** 731.
24. Landolt-Börnstein, Zahlenwerte und Funktionen, 6. Auflage, Vol. II (1969).